ELSEVIER

Biophysical Chemistry 74 (1998) 175–186

Biophysical Chemistry

Conformation induction in melanotropic peptides by trifluoroethanol: fluorescence and circular dichroism study

Kasturi Mukhopadhyay, Soumen Basak*

Nuclear Chemistry Division, Saha Institute of Nuclear Physics, 1 / AF Bidhannagar, Calcutta 700064, India

Received 30 January 1998; received in revised form 27 May 1998; accepted 3 June 1998

Abstract

Conformation induction in the two related peptides, α-melanocyte stimulating hormone (α-MSH) and δ-melanocyte stimulating hormone (δ-MSH), have been studied in solvent media containing varying percentages of the membrane-mimetic solvent 2,2,2-trifluoroethanol (TFE) using fluorescence and circular dichroism (CD) spectroscopy. Singular value decomposition (SVD) analysis of the CD spectra at different TFE concentrations showed that these spectra can be described as linear combinations of only two distinct *basis spectra*, corresponding to the peptides in the random-coil and 'folded' conformations. For α-MSH the spectrum of the folded state is very similar to the standard spectrum of the α-helix, while that for δ-MSH has partial resemblance to the helical spectrum. Fitting the data on ellipticity (at 222 nm) as a function of TFE volume fraction to an equation based on a two-state model describing TFE-induced conformation induction in the peptides gave values of (1.1 ± 0.4) and (4.2 ± 0.5) kcal mol^{-1} for α-MSH and δ-MSH, respectively, for the free energy of equilibrium between the helix and coil forms in water. Measurement of fluorescence emission parameters (emission maximum, quantum yield, steady-state anisotropy and mean excited-state lifetime) indicated that the microenvironment around the single tryptophan residues of both peptides changes in like manner with increasing concentration of TFE in the solvent. The similarity of fluorescence behaviour of the peptides suggests that their Trp fluorophores do not participate in secondary structure formation in TFE.

Keywords: Melanocyte stimulating hormone; Trifluoroethanol; Fluorescence; Circular dichroism; Singular value decomposition; α-Helix

* Corresponding author. Tel.: +91 33 3370605; fax: +91 33 3374637; e-mail: sbasak@hp1.saha.ernet.in

0301-4622/98/$19.00
PII S0301-4622(98)00177-X

1. Introduction

α-Melanocyte stimulating hormone (α-MSH or α-melanotropin) is secreted by the intermediate lobe of vertebrate pituitaries and has been shown to act on vertebrate pigmentation, adrenal cell stereogenesis and neural functioning related to learning and behaviour [1,2]. It is a linear tridecapeptide with a sequence identical with that of the 13 N-terminal amino acid residues of adrenocorticotropic hormone (ACTH); additionally, its N-terminus is acetylated and the peptide chain terminates with a valine carboxamide group. δ-Melanocyte stimulating hormone (δ-MSH) is a peptide fragment within the precursor protein (pro-opiomelanocortin) of α-MSH and exhibits considerable sequence similarity to it [3], although it has no reported melanotropic activity. It is a heptapeptide containing methionine and tryptophan residues at positions characteristic of the MSH sequence and shares with α-MSH serine and glutamic acid residues at equivalent positions:

α-MSH: Ac-Ser-Tyr-Ser-Met-Glu-His-Phe-Arg-Trp-Gly-Lys-Pro-Val-NH_2

δ-MSH: Ser-Met-Glu-Val-Arg-Gly-Trp

Structure–function relationships for α-MSH have been studied by analysis of the biological activities of a number of its structurally or stereochemically modified analogues and fragments. These studies identified the central tetrapeptide segment His^6-Phe^7-Arg^8-Trp^9 as the minimal melanotropic message sequence of α-MSH which is absolutely required for its biological activity [4]. However, there is a lack of consensus about the nature of the secondary structure adopted by α-MSH in its active state. Various groups have proposed that the biologically active conformation of α-MSH may contain either a β-turn [5] or an α-helix [2] within the active sequence for optimum interaction with the melanocyte receptor. Molecular dynamics studies have also suggested that α-MSH may prefer a reverse turn conformation centred about the Phe^7 residue and that it would form amphiphilic conformations with the charged groups on one surface of the molecule and the lipophilic groups on another [6].

The organic solvent 2,2,2-trifluoroethanol (TFE) is well-known for its ability to induce secondary structures in peptides and proteins dissolved in it [7–9]. Although the precise mechanism of such conformation induction remains unclear, it is generally agreed upon that structure formation occurs due to enhanced intramolecular hydrogen-bonding capabilities of peptides located in TFE-rich environments. With few exceptions, the addition of TFE to aqueous peptide solutions is known to stabilize the α-helical conformation. However, it has also been found that identical peptide sequences form α-helices in TFE and β-strands in micellar media, thus establishing the importance of environment (i.e. solvent type) in determining secondary structure [10,11]. Thus, TFE is generally regarded as a helix-promoting solvent, although it has been proposed that a requirement for helix propensity inherent in the primary amino acid sequence is necessary for the host peptide to develop this secondary structure [9].

A number of studies have shown that the conformational tendencies of peptides in TFE are similar to those which occur when the peptides interact with receptors or biomembranes (see, e.g. Öhman et al. [12]). In the present work we report a study of the evolution of secondary structures in the MSH peptides upon incremental addition of TFE to their aqueous solutions, using circular dichroic (CD) spectroscopy in the far-ultraviolet region to monitor secondary structures of the peptide backbones. Fluorescence emission properties provide a sensitive means of obtaining information on local structures of the peptides around the emitting fluorophores [13]. We have also measured the steady-state and time-resolved emission properties of the single Trp fluorophores of the peptides in presence of TFE, with the eventual aim of finding correlations between the structural information thus obtained on the local and the global scales. Our results show that TFE induces both peptides to adopt folded structures which in the case of α-MSH is very likely helical, whereas the fluorescence parameters of both peptides exhibit similar behaviour as the

fraction of TFE in the solvent is changed. The likely reason for this apparent lack of correlation between the structural information obtained using the two spectroscopic methods is that structure formation does not involve the Trp fluorophores in either peptide.

2. Materials and methods

High purity α-MSH and δ-MSH were purchased from Sigma Chemical Co. (St Louis, MO). TFE (Gold Label) was purchased from Aldrich (USA). All chemicals were used as received. Peptide concentrations were determined spectrophotometrically, using molar extinction coefficients at 280 nm of 6.65×10^3 M^{-1} cm^{-1} for α-MSH [14] and 5.6×10^3 M^{-1} cm^{-1} for δ-MSH.

Absorption measurements were carried out on a Shimadzu UV-2101PC spectrophotometer. Fluorescence emission spectra, corrected for non-uniform wavelength response of the monochromators and the photomultiplier detector, were recorded on a Hitachi F-4010 spectrofluorometer, using excitation at 280 nm for δ-MSH and *N*-acetyl-tryptophanamide (NATA) (and at 295 nm for α-MSH (to selectively excite its tryptophan residue). Excitation and emission bandwidths of (3, 1.5), (5, 5) and (5, 5) nm were used to measure wavelength at emission maximum quantum yield and steady-state anisotropy, respectively. Peptide-free TFE–water mixtures were used as reference blanks in all absorption and emission measurements. Quantum yields (ϕ_p) of peptides were determined relative to that of a solution of L-tryptophan at pH 7.0 (ϕ_{trp}) by comparing the area (A_p) under its emission spectrum with that for L-trp (A_{trp}). For calculating ϕ_p, ϕ_{trp} was taken to be 0.14 [15]. Steady-state anisotropies were measured on the Hitachi F-4010 using L-format optics. All experiments were performed at 25°C.

Fluorescence total emission intensity decay measurements were carried out on a fluorescence lifetime spectrometer assembled in our laboratory with components from Edinburgh Analytical Instruments (EIA, UK) and EG&G ORTEC (USA) and operated in the time-correlated-single-photon-counting mode. Excitation was provided by a pulsed high-pressure (1.5 atm) N_2-lamp operating at 25 kHz repetition rate, the pulse profile having a FWHM of 1.3 ns. Tryptophan excitation was provided by the 297-nm N_2-line, while emission decay profiles were monitored at 350 nm. Slits with 16 nm bandpass were used in both excitation and emission channels. Intensity decay profiles were fitted to the series:

$$I(t) = \Sigma_i A_i \exp(-t/\tau_i) \quad (1)$$

where A_i represents the fractional contribution to the time-resolved decay of the component with lifetime τ_i. The decay parameters were recovered using a software package supplied by EIA, implementing a non-linear least-squares iterative fitting procedure based on the Marquardt algorithm [16]. Mean lifetimes $\langle\tau\rangle$ for biexponential decays were calculated using the equation [17]:

$$\langle\tau\rangle = \alpha_1\tau_1 + \alpha_2\tau_2 \quad (2)$$

where the fractional amplitude α_i corresponding to the lifetime τ_i is given by:

$$\alpha_i = A_i\tau_i/(A_1\tau_1 + A_2\tau_2), \qquad i = 1, 2 \quad (3)$$

CD spectra were recorded at room temperature using a Jasco J-720 spectropolarimeter (calibrated with *d*-10-camphorsulfonic acid) and a cylindrical quartz cuvette of path length 2 mm. The following scan parameters were used: 1-nm bandwidth, 2 s response time, 0.1-nm step resolution and 20 nm min^{-1} scan speed. Each spectrum was an average of five continuous scans, measured between 190 and 250 nm. The acquired spectra were corrected by subtracting blank runs on peptide-free TFE–water mixtures of the appropriate compositions, subjected to noise-reduction analysis, and presented as mean residue molar ellipticity in degree cm^2 $dmol^{-1}$.

Singular value decomposition (SVD) analysis: To help identify the number of distinct spectra contributed by different peptide conformations which evolve as the volume fraction of TFE in solvent is changed, the CD spectral data were subjected to SVD analysis [18–20]. In general, a measured CD spectrum is a sum of several overlapping compo-

nents each of which is characteristic of the peptide in a given conformation. The relative mixtures of these components in the measured spectra change with changing solvent composition (condition variable). The use of SVD allows us to separate the component spectra, thereby leading to a knowledge of the number and nature of the most important individual components.

For this analysis, the complete set of CD spectra over the total range of TFE concentrations was arranged into an $m \times n$ matrix **A**, of which each column represents a digitized spectrum ($m = 601$ corresponding to a wavelength step-size of 0.1 nm over the range 190–250 nm common to all spectra) while the different columns correspond to varying solvent compositions. The matrix **A** thus represents the entire information content of the spectral series being analyzed for each peptide. The SVD procedure consists of expressing the matrix **A** in the product form $\mathbf{A} = \mathbf{USV}^{\mathbf{T}}$, where **U** is an $m \times n$ matrix of orthogonal *basis vectors*, **S** is a diagonal matrix of *singular values* and $\mathbf{V}^{\mathbf{T}}$ is an $n \times n$ matrix of *amplitudes*. The columns of the product matrix **US** form the desired *basis spectra*. These are themselves linear combinations of the measured spectra and under suitable conditions represent the contributions of the distinct chemical or conformational species. The magnitude of each singular value determines the relative importance of the corresponding basis spectrum in reproducing the original CD spectra. They are arranged in order of descending magnitude in **S** such that $\mathbf{S} = \mathrm{diag}(s_1, s_2, ..., s_n)$ where $s_1 \geq s_2 \geq s_n \geq 0$. The utility of SVD analysis lies in projecting out the minimum number of basis spectra (the most significant ones) which can be recombined linearly in appropriate proportions to best reproduce (in a least-squares sense) the measured spectral set, i.e. the matrix **A**. The coefficients of this recombination are contained in the *amplitude matrix* **V**, of which the columns fit the original spectra to the basis spectra and the rows fit the basis spectra to the original spectra. Thus the elements of the ith row of **V** represent the relative linear contributions of all the basis spectra in the ith original spectrum, while the elements of the ith column of **V** represent the relative contributions of the ith basis spectrum in the measured spectra (over the whole range of the condition variable).

For perfect, noiseless data the number of non-zero singular values equals the number of independent spectral components in the data set. In the presence of noise the number of independent species that make significant contributions can be identified from a comparison of the relative magnitudes of singular values and the autocorrelations of the basis or amplitude vectors. The latter constitute useful measures of the signal-to-noise ratio of given columns of **U** or **V** and are defined as follows [18,20]:

$$C(X_i) = \sum_j X_{j,i} X_{j+1,i} \tag{4}$$

where $X_{j,i}$ represents the jth element of the ith column of the **U** or **V** matrix. Since the columns of **U** and **V** are all normalized to unity, C lies between -1 and $+1$. Typically, a large gap in the magnitude of the singular values can indicate the transition from the significant ('signal') to the irrelevant ('noise') components. Components thus selected may be further screened on the basis of the autocorrelations calculated according to Eq. (4). For components with good signal-to-noise ratio C should be close to unity, whereas noisy components would yield much smaller (and possibly negative) values of C. The SVD analysis presented here was carried out using a standard FORTRAN subroutine [21].

3. Results

3.1. Circular dichroism

The CD spectrum of α-MSH (37 μM, 0.06 mg ml^{-1}) in 0.05 M, pH 7.4 phosphate buffer is that of a peptide predominantly in random-coil form, having a strong negative maximum centred at 198 nm arising out of the $\pi \rightarrow \pi^*$ transition of the amide bond (Fig. 1). The nature of the spectrum remains unaltered under a 10-fold dilution of the peptide concentration (data not shown). The spectrum changes noticeably and rapidly with addition of TFE in the solvent. The $\pi \rightarrow \pi^*$ transition band splits into a dominant positive peak

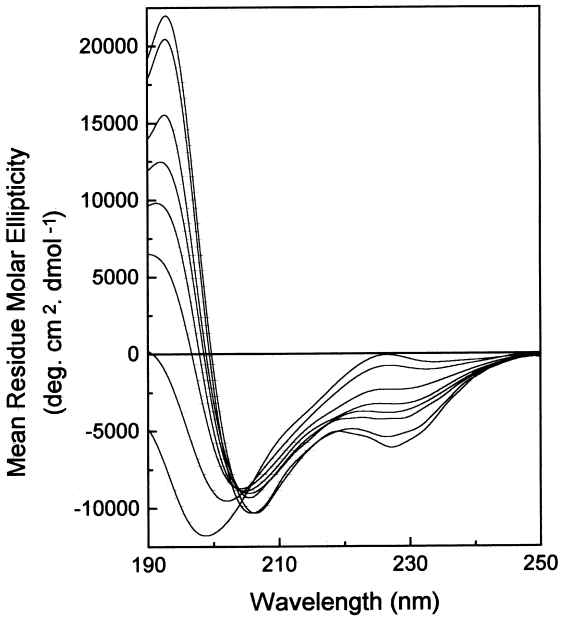

Fig. 1. CD spectra of α-MSH in mixtures of 0.05 M, pH 7.4, phosphate buffer and TFE. Successive traces with decreasing Θ_{222} are for 0, 25, 50, 60, 70, 80, 90 and 100% TFE (v/v), respectively.

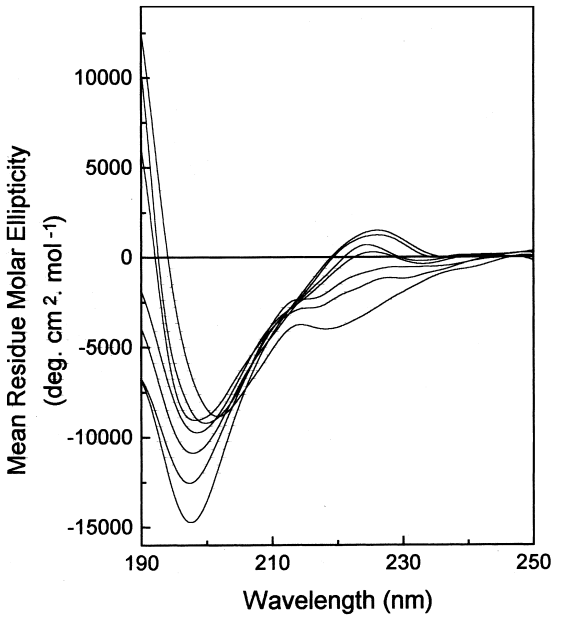

Fig. 2. CD spectra of δ-MSH in TFE–water mixtures. Successive traces with decreasing Θ_{222} are for 0.05 M phosphate buffer (pH 7.4), 25, 50, 70, 80, 90 and 100% TFE (v/v), respectively.

around 193 nm, while the original negative band at 198 nm red-shifts to 206 nm. In addition, the $n \rightarrow \pi^*$ transition band of the amide starts to show up as another negative band around 226 nm. These results are in good agreement with those of Greff et al. [22], who reported formation of α-helical structure in the peptide fragment ACTH(1–14) (whose first 13 residues are identical with those of α-MSH) dissolved in 100% TFE.

The CD spectra of δ-MSH (34 μM, 0.03 mg ml^{-1}) in phosphate buffer and in TFE-enriched solvents are shown in Fig. 2. The buffer spectrum is typical of a peptide in random conformation, with a large negative extremum at 198 nm and a small positive peak at 228 nm. Changes occur in this spectrum in response to the addition of TFE, the most significant of which are for TFE volume fractions 60% (v/v) and higher. At 80% TFE, the negative maximum shifts to 203 nm while a strong positive contribution appears below 195 nm. In addition, the weak positive peak around 228 nm gives way to an emerging second negative extremum around 220 nm.The magnitude of ellipticity decreases from 14 697° cm^2 $dmol^{-1}$ at 198 nm in buffer to 8643° cm^2 $dmol^{-1}$ at 203 nm in 100% TFE. Unlike in the case of α-MSH, however, there is no clear isodichroic in these spectra.

To identify the nature of the additional spectra contributed by the presence of TFE in the solvent, a SVD analysis of the complete set of measured CD spectra (covering the range of TFE volume fractions from 0 to 100%) was performed for each peptide. The singular values obtained for the (601×8) matrix **A** for α-MSH and the (601×7) matrix **A** for δ-MSH are listed in Table 1. Also shown there are the autocorrelations of the amplitude vectors represented by the columns of **V**, i.e. $C(X_i)$ with $X = \mathbf{V}$. Examination of these entries shows that for both peptides the first two singular values and autocorrelations dominate over the remaining ones. The basis spectra corresponding to these singular values (i.e. the first two columns of the matrix product **US**) are shown in Fig. 3(a) and 3(b) for α-MSH and δ-MSH, respectively. For comparison, these figures also show the basis spectra having the next most significant

Table 1
Singular values and correlations of SVD amplitude vectors for the far-UV CD spectra of the peptides in TFE–water mixtures

Component No.	α-MSH		δ-MSH	
	Singular value	Amplitude autocorrelation	Singular value	Amplitude autocorrelation
1	391 295	0.84	298 928	0.83
2	182 686	0.61	108 427	0.56
3	5863	0.47	15 286	−0.04
4	4338	−0.27	5638	−0.03
5	2941	−0.23	3321	−0.71
6	2165	−0.62	1851	−0.74
7	832	−0.83	1520	0.14
8	994	0.02		

singular value. It is evident that only the first two basis spectra can be classified as 'signal', the rest falling in the category of 'noise'.

Fig. 4a,b show the amplitudes of the two most prominent basis spectra plotted against the nominal TFE volume fraction (condition variable) for α-MSH and δ-MSH, respectively. These results can be interpreted as follows: the CD spectrum measured in a mixed solvent containing a given TFE volume fraction can be best approximated by a linear combination of the two basis spectra shown in Fig. 3 using the coefficients of Fig. 4 for that TFE volume fraction.

3.2. Fluorescence

In order to obtain information on local structural changes of the peptides induced by TFE, we have examined their tryptophan emission properties while varying the hydration conditions of the solvent. To dissociate the effects of the solvent medium on Trp itself from those on the peptides, the fluorescence of the model compound NATA was also studied under the same set of conditions [13]. It was found that in going from an aqueous buffer to 100% TFE, NATA exhibits a 3-nm *blue shift* of its emission peak (353–350 nm), a more than fourfold *decrease* in quantum yield (0.14–0.03), an *increase* of anisotropy from 0 to 0.03 and a more than threefold *decrease* in the excited-state lifetime (3–1 ns). Fig. 5a–c present a summary of the changes in three steady-state emission parameters — emission maximum,

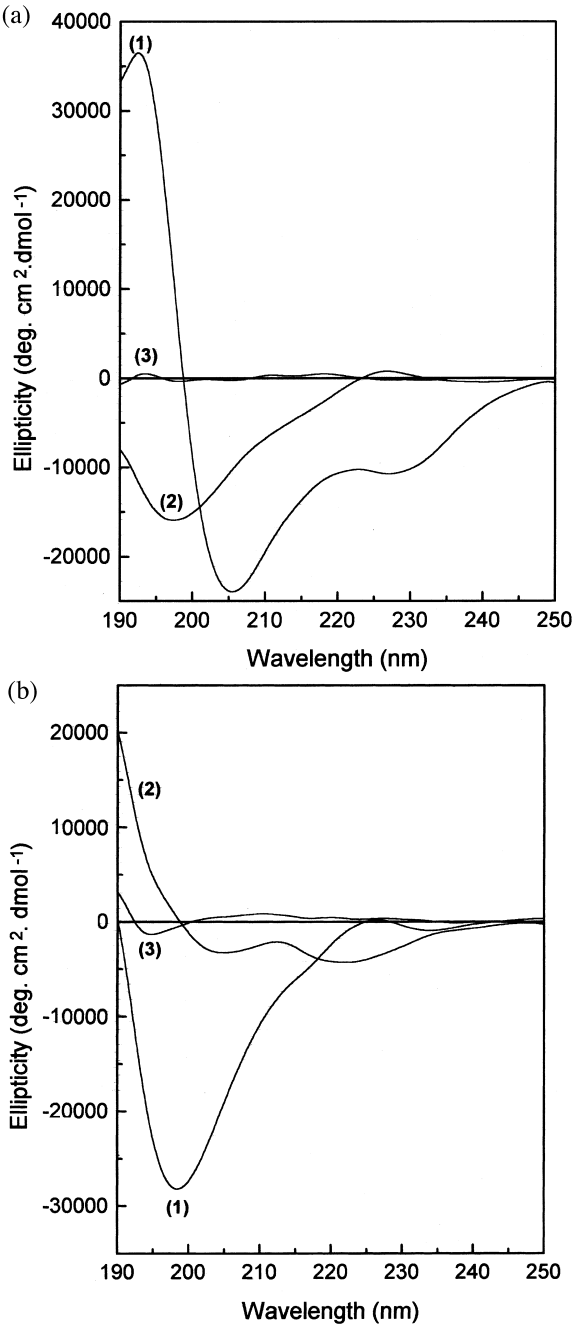

Fig. 3. Plots of the basis spectra corresponding to the three largest singular values [marked (1), (2) and (3), respectively] for (a) α-MSH and (b) δ-MSH.

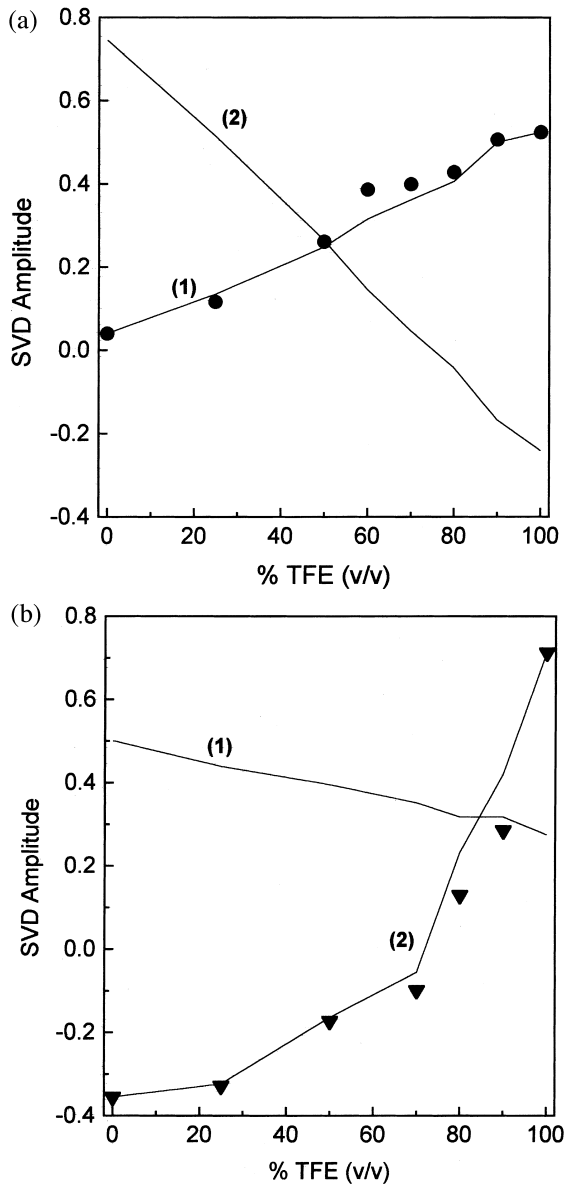

Fig. 4. Plots of the SVD amplitude vectors for the two most prominent basis spectra vs. TFE volume fraction for (a) α-MSH and (b) δ-MSH. Also shown in each panel are plots of Θ_{222}, normalized to have the same extreme values as the corresponding amplitudes for the 'folded' state, (see Section 4 of text) for (a) α-MSH (●) and (b) δ-MSH (▼).

quantum yield and anisotropy — with changing concentration of TFE. The results for the peptides should be compared with those for NATA in solvents of identical composition. A change of solvent from phosphate buffer to TFE produces a somewhat larger blue shift (5 nm) of the emission peak for both peptides. The reduction of quantum yield is nearly the same for both, but approximately half as much as for NATA. As a result, the 'effective' quantum yields of the peptides, normalized with respect to that of NATA by dividing by the ratio of the quantum yield of NATA in the same mixed solvent to that in water, *increase* in going from water to TFE, by factors of approximately two. Steady-state anisotropies also increase substantially, from ~ 0 in water to 0.07–0.08 in TFE, much larger than that observed for NATA under the same conditions.

Total emission intensity decay measurements showed that double exponential fits were required to satisfactorily fit the data for both peptides at all water–TFE compositions, although NATA always exhibited monoexponential fluorescence decay. The lifetimes of NATA in pH 7.4, 0.05 M phosphate buffer and in 100% TFE were 3 ns and 1 ns, respectively. Table 2 shows that for both peptides the mean excited-state lifetimes decrease with increasing proportion of TFE in the solvent. In addition to its effect on the peptide conformation TFE also quenches Trp fluorescence, as indicated by the result of lifetime measurements on NATA. The effect of this general solvent quenching can be eliminated by dividing the mean lifetimes of the peptides by the ratio of the lifetimes of NATA in the same mixed solvent and in water. The mean fluorescence lifetime, thus normalized, actually *increases* for both peptides upon transfer from water to TFE: for α-MSH $\langle\tau\rangle_n = 2.7$ ns in water and 4.5 ns in 100% TFE, while for δ-MSH $\langle\tau\rangle_n = 2.1$ ns in water and 3.0 ns in 100% TFE, where $\langle\tau\rangle_n$ is the mean lifetime normalized with respect to that of NATA. For both peptides, this increase of the 'normalized' mean lifetime is about the same as that of the 'effective' quantum yield in going from water to pure TFE.

Changes in fluorescence lifetime ($\langle\tau\rangle$) can lead to changes in anisotropy (r), these two parameters being related through Perrin's equation [17]:

$$\tau_c = \langle\tau\rangle/(r_0/r - 1) \quad (5)$$

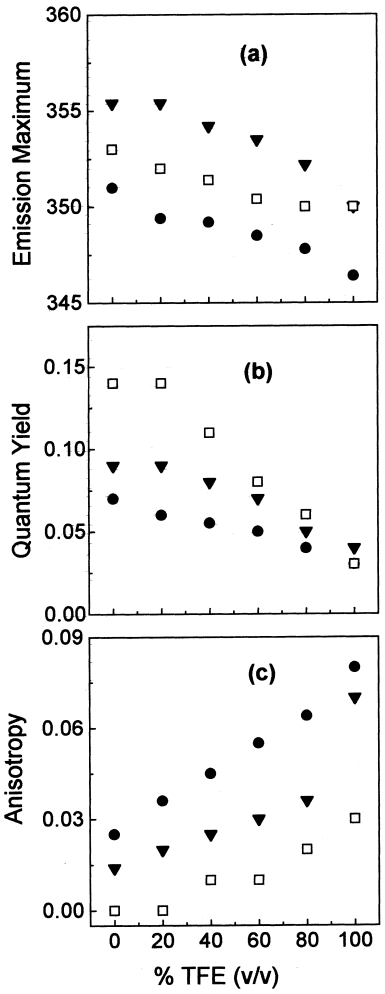

Fig. 5. Variation of tryptophan steady-state emission parameters for α-MSH (●), δ-MSH (▼) and NATA (□) with volume fraction of TFE: (a) emission (maximum); (b) quantum yield; and (c) anisotropy.

where r_0 is the limiting anisotropy in a medium of high viscosity and at low temperature and τ_c is the correlation time characteristic of rotational diffusion of the fluorophore. τ_c is a more direct measure than anisotropy of the resistance offered by the medium to the degrees of freedom of the fluorophore. In order to delineate the effect of changing fluorescence lifetime on the nature of the fluorophore environment, we have calculated τ_c, in the mixed solvents (Table 2) using previously determined values of r_0 for NATA and the Trp in these peptides [23]. For both peptides the correlation time showed a definite increase in going from water to TFE (0.4–1.0 ns for α-MSH, 0.2–0.6 ns for δ-MSH), which was larger than that calculated for the model compound NATA ($\sim$ 0–0.2 ns).

4. Discussion

4.1. Analysis of CD spectra

CD spectra show that neither peptide has the tendency for formation of a well-defined secondary structure in aqueous solution. In the presence of TFE, the spectra of both peptides exhibit major changes differing in their dependence on TFE concentration. SVD analysis of the CD data yielded two prominent basis spectra which contribute to the measured spectra for each peptide (Fig. 3). Of the two, one clearly represents each peptide in a random conformation [spectrum marked (2) for α-MSH and (1) for δ-MSH]. The features of the second basis spectrum for α-MSH [marked (1)] — a strong positive peak at 192 nm and twin negative maxima at 206 and 226 nm — recall the classical spectrum of proteins in the right-handed α-helical conformation [24]. That the magnitudes of the two negative maxima are unequal is not unusual for short helical peptides, having been observed previously for the peptides bombesin and spantide [25,26]. The features of the other basis spectrum for δ-MSH [marked (2)] do not match those of the standard α-helical CD spectrum quite as well, although their sign and location are approximately correct. It is possible that due to the short length of this peptide the helix in it is only partially formed (less than a full turn), thus contributing a non-standard spectrum.

It should be mentioned that since the spectra for δ-MSH (Fig. 2) do not have an isodichroic point, in principle there exists the possibility of contributions from other types of secondary structures (e.g. β-type). In fact, the basis spectrum marked (3) in Fig. 3b could have been taken to represent such a structure, but for its negative correlation coefficient (Table 1). Perhaps these additional contributions are weak enough to be

Table 2
Total emission intensity decay parameters of tryptophan fluorescence for the peptides dissolved in mixtures of TFE and 0.05 M, pH 7.4, phosphate buffer

Sample	% TFE	τ_1 (ns)	α_1 (%)	τ_2 (ns)	α_2 (%)	$\langle\tau\rangle$ (ns)	τ_c (ns)
α-MSH	0 (buffer)	3.2	79.3	0.9	20.7	2.7	0.37
	25	2.8	72.6	0.9	27.4	2.3	0.50
	50	2.7	65.3	0.9	34.7	2.1	0.65
	75	2.4	61.0	0.8	39.0	1.8	0.77
	100	2.8	34.5	0.8	65.5	1.5	0.95
δ-MSE	0 (buffer)	2.5	78.4	0.5	21.6	2.1	0.16
	25	2.5	74.9	0.5	25.1	2.0	0.24
	50	2.3	69.9	0.5	30.1	1.8	0.30
	75	2.0	55.5	0.5	44.5	1.3	0.29
	100	1.9	34.7	0.5	65.3	1.0	0.56
NATA	0 (buffer)	3.0				3.0	0.0
	100	1.0				1.0	0.20

Notes. Decay profiles were fitted to the expression $I(t) = A_1 \exp(-t/\tau_1) + A_2 \exp(-t/\tau_2)$ for the peptides; for NATA, the decay law was single exponential. For definitions of amplitudes α_i, mean lifetime $\langle\tau\rangle$ and rotational correlation time τ_c, see text. Estimated errors in $\langle\tau\rangle$ and τ_c are ± 0.1 ns and ± 0.05 ns, respectively.

masked by the noise and are 'averaged out' by the SVD analysis. Similar considerations apply to the case of α-MSH; however, the spectra in Fig. 1 do have an approximate isodichroic point around 203 nm, and the absence of an 'exact' isosbestic could be due to errors in the determination of peptide concentrations.

The plots of SVD amplitudes (Fig. 4) allow a comparison of TFE-induced secondary structure evolution in the two peptides. As already pointed out on the basis of singular values and amplitude autocorrelations, which showed a clear break after the second component for both peptides in Table 1, only two major conformational species for each can be concluded to exist in the presence of TFE. Changes in the CD spectra with increasing TFE concentration can be accounted for by decreasing proportions of peptides in the random-coil state and increasing proportions in the folded state, as inferred from Fig. 4. For α-MSH, TFE-induced folding occurs more or less uniformly with a mid-point at approx. 50% (v/v) TFE (Fig. 4a). For δ-MSH, there appears to be an 'inductive region' of TFE concentrations where the amplitude of the folded species changes relatively slowly, followed by a region of steep increase having its mid-point at 85% (v/v) TFE (Fig. 4b). An interesting correlation has been found by plotting the variation of the ellipticity at 222 nm (Θ_{222}), normalised to have the same values at 0 and 100% TFE (v/v) as the SVD amplitude of the folded conformation, against the TFE volume fraction (Fig. 4a,b). For both peptides, the variation of the normalised Θ_{222} closely follows that of the amplitudes of the folded states [(1) for α-MSH and (2) for δ-MSH]. As the magnitude of Θ_{222} is traditionally taken to indicate the extent of helix formation in peptides, this correlation supports the possibility of the TFE-induced folded states being helical in the present case.

The thermodynamics of TFE-induced conformational transition in proteins can be analysed by treating it in a manner similar to the protein denaturation process [27,28]. The spectra of α-MSH (Fig. 1) have an approximate isodichroic point at 203 nm suggesting that the structural transition is a two-state process, involving contributions from only two distinct conformations (in this case, random-coil and most likely helix). This idea is also supported by the result of the SVD analysis described above, which yielded only two independent basis spectra that could reproduce all the measured CD spectra. Assuming that the folding–unfolding transition of peptides in

TFE can be described in the framework of the same two-state model as that used to describe the effects of urea and guanidinium chloride as protein denaturants, the following relation between the ellipticity and the percent volume fraction of TFE in the solvent ([TFE]) has been derived [27]:

$$\Theta = \frac{\Theta_F + \Theta_U \exp\{-(m[\mathrm{TFE}] - \Delta G_{\mathrm{water}})/RT\}}{1 + \exp\{-(m[\mathrm{TFE}] - \Delta G_{\mathrm{water}})/RT\}} \quad (6)$$

where Θ_F is the ellipticity of the peptide at maximal TFE concentration and Θ_U that in the random conformation, $\Delta G_{\mathrm{water}}$ the standard free energy of equilibrium between the two forms in water, m a proportionality constant between the free energy and [TFE] ($\Delta G_F = \Delta G_{\mathrm{water}} - m$ [TFE]), R the gas constant and T the temperature. We have fitted the measured values of the ellipticity at 222 nm (which is traditionally taken to represent the extent of helix formation) for α-MSH as a function of the volume fraction of TFE to Eq. (6), while treating Θ_F, Θ_U, m and $\Delta G_{\mathrm{water}}$ as unknowns. Because of the small number of data points spanning the large range of TFE concentrations, a family of curves could be made to fit the data, leading to wide variations in the fitting parameters. A typical fit is shown in Fig. 6, yielding a value of (1.1 ± 0.4) kcal mol^{-1} (1 cal = 4.184 J) for the free energy of unfolding of the peptide in water ($\Delta G_{\mathrm{water}}$). The large uncertainty reflects the variability of the fitting parameters. This value of $\Delta G_{\mathrm{water}}$ agrees quite well with that obtained from TFE-titration experiments for the N-terminal fragment of Barnase, which is a peptide of the same length as α-MSH [27]. Although the spectra for δ-MSH do not exhibit an isodichroic point, we have nevertheless extended the above analysis to this peptide. Fig. 6 shows the result of fitting the ellipticity data for δ-MSH to Eq. (6), yielding a value of (4.2 ± 0.5) kcal mol^{-1} for $\Delta G_{\mathrm{water}}$. This $\Delta G_{\mathrm{water}}$ value indicates higher stabilisation of the folded structure in δ-MSH than in α-MSH, which is surprising since structure formation ensues at a much lower TFE concentration in the latter than in the former (Figs. 1 and 2).

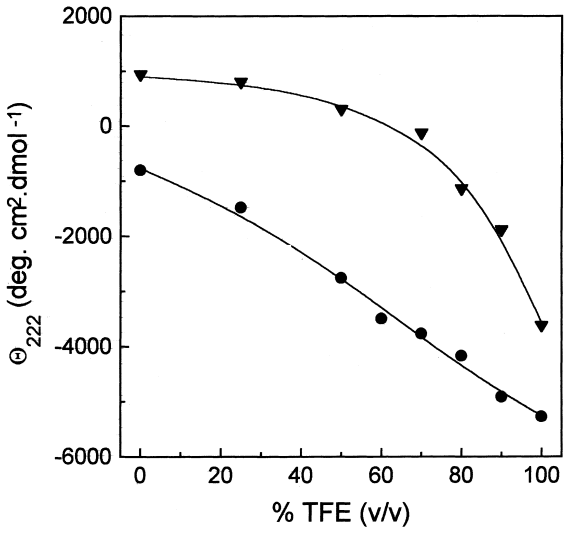

Fig. 6. Variation of Θ_{222} vs. [TFE] for α-MSH (●) and δ-MSH (▼). The continuous lines represent best fits of the data to Eq. (6) of text.

4.2. Fluorescence

Fig. 5a shows that both peptides have their emission maxima in TFE blue shifted from those in the buffer by same amounts (5 nm) that are larger than that obtained for NATA. This points to increasingly hydrophobic environments for the tryptophans as the proportion of TFE is increased. Simultaneous enhancement of the 'effective' quantum yields and 'normalized' mean lifetimes (as explained in the Section 3) indicate that some deactivation pathways of the excited fluorophores are blocked out. Increasing steady-state anisotropies (Fig. 5c), which are much higher than that observed for NATA, indicate that the effect of replacing water with TFE is to make the microenvironment around the tryptophans more and more rigid. That the enhanced rigidity of the environment was not an artefact of the decreased fluorescence lifetime in TFE-rich solvents (leading to the observed increase in steady-state anisotropy) was proved by the increase in the calculated values of the correlation time τ_c (Table 2), it being a direct measure of the resistance of the medium to rotational diffusion of the fluorophore. The fluorescence data are thus consistent with the general trend emerging from CD

measurements that the presence of TFE leads to structure induction in the peptides.

The lack of correlation between the structural information obtained using CD and fluorescence can be explained by recalling the fact that while CD monitors the average secondary structure of the peptide backbone, fluorescence probes only the local structure and interactions around the tryptophan moiety. Agreement between inferences drawn from these two techniques thus depends on tryptophan being part of the region of the peptide which contains the structural feature. Though the observed conformational change is much more pronounced for α-MSH than δ-MSH as revealed by the CD data, Trp emission parameters show the same change for both peptides. This suggests that secondary structure formation does not involve the tryptophan residues in either peptide, in agreement with the result of structure-prediction algorithms [29] that helix-forming potential is clustered among the residues Met^4-Glu^5-His^6-Phe^7 in α-MSH and Met^2-Glu^3-Val^4 in δ-MSH. Changes in fluorescence emission parameters only reflect the increasingly anhydrous nature of the solvent medium caused by replacement of water by TFE.

5. Concluding remarks

Small peptides, such as hormones, exhibit better defined secondary structures in a hydrophobic environment, which are usually quite different from the random coil-like structures seen in aqueous solution. These better defined structures may mimic the functional ones, existing when the peptide interacts with a receptor or a biomembrane [30,31]. The aim of the present study was to investigate how changing hydrophobicity, brought about by varying the concentration of the cosolvent TFE, affects secondary structure stabilization of the two related melanotropic peptides α-MSH and δ-MSH. SVD analysis of CD spectra in presence of TFE suggests that the nature of the folded structure adopted by α-MSH is helical (Fig. 3a); for δ-MSH, too, the basis spectrum looks approximately helical (Fig. 3b). It is tempting to conclude from this that the active conformation of the message segment of α-MSH at its receptor site would be a helix. However, it is worth remembering that since TFE specifically promotes helix formation in peptides, there is no certainty that the helical conformation would also be formed in hydrophobic environments in vivo. The fluorescence data suggest that the Trp residue of neither peptide forms part of its structure-forming segment.

Acknowledgements

The authors thank Professor S.K. Ghosh for access to the JASCO J-720 spectropolarimeter.

References

[1] R. Schwyzer, Ann. N. Y. Acad. Sci. 297 (1977) 3.
[2] R. Schwyzer, Helv. Chim. Acta 69 (1986) 1685.
[3] S. Nakanishi, A. Inoue, T. Kita, et al., Nature 278 (1979) 423.
[4] A.S. Ito, A.M. de L Castrucci, V.J. Hruby, M.E. Hadley, D.T. Krajcarski, A.G. Szabo, Biochemistry 32 (1993) 12264.
[5] T.K. Sawyer, V.J. Hruby, P.S. Darman, M.E. Hadley, Proc. Natl. Acad. Sci. USA 79 (1982) 1751.
[6] V.J. Hruby, W. Kazmierski, B.M. Petit, F. Al-Oeidi, in: M. Chretien, K.W. Mckerns (Eds.), Molecular Biology of Brain Endocrine Peptidergic Systems, Plenum Press, New York, 1988, p. 13.
[7] J.W. Nelson, N.R. Kallenbach, Proteins: Struct. Func. Gen. 1 (1986) 211.
[8] J.W. Nelson, N.R. Kallenbach, Biochemistry 28 (1989) 5256.
[9] F.D. Sonnichsen, J.E. Van Eyk, R.S. Hodges, B.D. Sykes, Biochemistry 31 (1992) 8790.
[10] L. Zhong, W.C. Johnson, Proc. Natl. Acad. Sci. USA 89 (1992) 4462.
[11] D.V. Waterhous, W.C. Johnson, Biochemistry 33 (1994) 2121.
[12] A. Öhman, P.-O. Lycksell, S. Andell, Ü. Langel, T. Bartfai, A. Gräslund, Biochim. Biophys. Acta 1236 (1995) 259.
[13] K.J. Willis, A.G. Szabo, Biochemistry 31 (1992) 8924.
[14] J. Gallay, M. Vincent, C. Nicot, M. Waks, Biochemistry 26 (1987) 5738.
[15] O.S. Wolfbeis, in: S.G. Schulman (Ed.), Molecular Luminescence Spectroscopy, Methods and Applications, Part 1, Wiley, New York, 1985, p. 167.
[16] P. Bevington, Data Reduction and Error Analysis for the Physical Sciences, McGraw Hill, New York, 1969.
[17] J.R. Lakowicz, Principles of Fluorescence Spectroscopy, Plenum Press, New York, 1983.
[18] R.I. Shrager, R.W. Hendler, Anal. Chem. 54 (1982) 1147.

[19] W.C. Johnson, in: B. Sedlacek (Ed.), Physical Optics of Dynamic Phenomena and Processes in Macromolecular Systems, Walter de Gruyter, Berlin, 1985, p. 243.
[20] E.R. Henry, J. Hofrichter, Methods Enzymol. 210 (1992) 129.
[21] W.H. Press, B.P. Flannery, S.A. Teukolsky, W.T. Vetterling, Numerical Recipes. The Art of Scientific Computing, Cambridge University Press, Cambridge, 1986, p. 52.
[22] D. Greff, F. Toma, S. Fermandjian, M. Low, L. Kisfaludy, Biochim. Biophys. Acta 439 (1976) 219.
[23] K. Bhattacharyya, S. Basak, Biophys. Chem. 47 (1993) 21.
[24] R.W. Woody, in: V.J. Hruby (Ed.), The Peptides, vol. 7, Academic Press, New York, 1985, p. 15.
[25] C. Di Bello, A. Scatturin, G. D'auria, et al., Biopolymers 31 (1991) 643.
[26] C. Di Bello, A. Scatturin, G. D'auria, et al., Biopolymers 31 (1991) 1397.
[27] J. Sancho, J.L. Neira, A.R. Fersht, J. Mol. Biol. 224 (1992) 749.
[28] A. Jasanoff, A.R. Fersht, Biochemistry 33 (1994) 2129.
[29] P.Y. Chou, G.D. Fasman, Biochemistry 13 (1974) 211.
[30] E.T. Kaiser, F.J. Kezdy, Science 223 (1984) 249.
[31] J.W. Taylor, G. Osapay, Acc. Chem. Res. 23 (1990) 338.